Accepted Manuscript

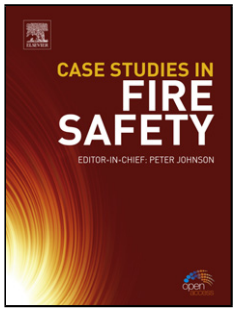

Title: Enhanced<!–<query id="Q1">Please check the Article Title for correctness and amend if necessary.</query>–> corrosion resistance of mild steel in 1 M HCl solution by trace amount of 2-phenyl-benzothiazole derivatives: Experimental, quantum chemical calculations and molecular dynamics (MD) simulation studies

Author: Zohreh Salarvand Mehdi Amirnasr Milad Talebian Keyvan Raeissi Soraia Meghdadi

PII: S0010-938X(16)31160-X
DOI: http://dx.doi.org/doi:10.1016/j.corsci.2016.11.002
Reference: CS 6929

To appear in:

Received date: 25-6-2016
Revised date: 6-11-2016
Accepted date: 12-11-2016

Please cite this article as: {http://dx.doi.org/

This is a PDF file of an unedited manuscript that has been accepted for publication. As a service to our customers we are providing this early version of the manuscript. The manuscript will undergo copyediting, typesetting, and review of the resulting proof before it is published in its final form. Please note that during the production process errors may be discovered which could affect the content, and all legal disclaimers that apply to the journal pertain.

ACCEPTED MANUSCRIPT

Enhanced corrosion resistance of mild steel in 1M HCl solution by trace amount of 2-phenyl-benzothiazole derivatives: experimental, quantum chemical calculations and molecular dynamics (MD) simulation studies

Zohreh Salarvand[a], Mehdi Amirnasr[a]*, Milad Talebian[b], Keyvan Raeissi[b], Soraia Meghdadi[a]*

[a]*Department of Chemistry, Isfahan University of Technology, Isfahan 84156-83111, Iran*

[b]*Department of Materials Engineering, Isfahan University of Technology, Isfahan 84156-83111, Iran*

***Corresponding authors: M. Amirnasr
S. Meghdadi
E-mail: amirnasr@cc.iut.ac.ir
smeghdad@cc.iut.ac.ir

ACCEPTED MANUSCRIPT

Graphical abstract

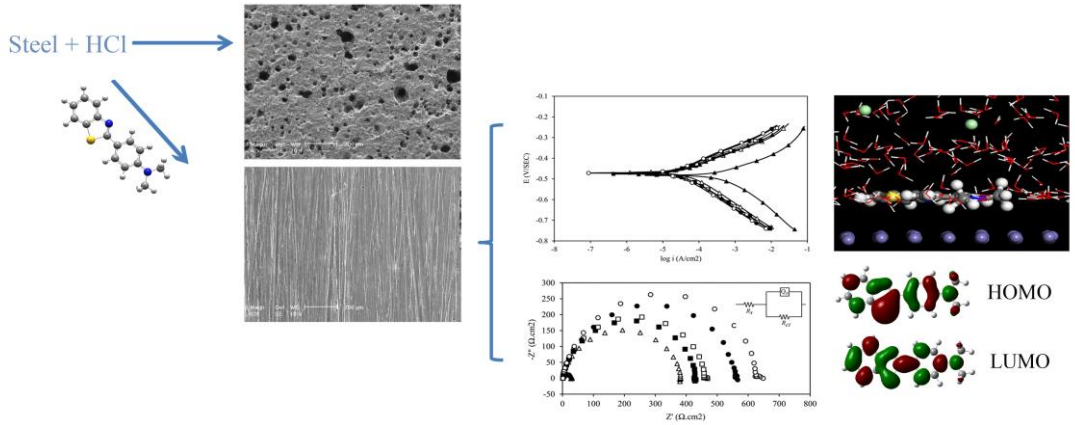

New Highlights

- **x** Green synthesized benzothiazole derivatives as inhibitors on mild steel in 1 M HCl.
- x The inhibition efficiency of N-dimethylbenzothiazole is >95% at 50 ppm (by weight).
- x These benzothiazole compounds act as mixed-type and adsorption inhibitors.
- x The conflict between experimental results and DFT is explained by MD simulation.
- x Both the molecular electronic and structure are effective in the inhibition process.

Abstract:

The inhibition performance of 2-• -hydroxylphenyl)benzothiazole, (**1**), 2-• -dihydroxyphenyl)benzothiazole, (**2**), and (4-benzothiazole-2-yl-phenyl)-dimethyl-amine, (**3**), has been investigated for mild steel in 1 M HCl. Notably, compound **3** shows 95% inhibition efficiency at 50 ppm (by weight) concentration. The adsorption of these compounds obeys the Langmuir adsorption isotherm with predominately chemisorption for **3** and comprehensive for **1** and **2**. Quantum chemical calculations predicted an inhibition order of **3**>**2**>**1**, is at odds with the experimental order due the structural effects. Molecular dynamic simulation revealed a nearly flat configuration for molecules on metal surface with negative binding energies in a sequence agreed by the experiments, **3**>**1**>**2**.

Keywords: Benzothiazole derivatives; Corrosion inhibitors; Mild steel; Electrochemical measurement; Quantum chemical calculation; MD simulation

ACCEPTED MANUSCRIPT

1. INTRODUCTION

The main problem of using iron alloys is their tendency to corrosion in contact with aggressive medium such as hydrochloric acid solution [1, 2]. Acid solutions are widely used in many industrial processes for pickling, cleaning, descaling, etching of metal and oil well acidizing. One of the practical and effective methods to reduce the corrosive attack on metallic material is application of inhibitors [2, 3]. The organic molecules used as inhibitor, are adsorbed on the metal VXUIDFHWKURXJKKHWHURDWRPVVXFKDV1632DQGWKHLUDURPDWLFULQJ[4-9]. This adsorption is either physical, by electrostatic interaction (physisorption) or chemical through covalent bond formation (chemosorption). Therefore, vast attention has been paid to the developing of new novel and cost effective organic inhibitors and studying their corrosion inhibition mechanism using several electrochemical techniques and surface analysis methods. The importance of the mechanism of corrosion inhibition and its relation with electronic and structural properties of the inhibitor molecules has also attracted attention to quantum chemical calculation [6, 10-16]. Quantum chemical studies, though instructive, are not usually adequate for rationalizing the experimental results, and in some cases, the results obtained from quantum chemical calculations do not correlate well with the experimentally determined inhibition efficiencies [17-19]. Modeling of an experiment by molecular dynamics (MD) simulation can provide a more realistic picture of the interfacial interactions between the metallic surface and the inhibitor molecules. As a result, the use of quantum chemical calculations supported by the molecular dynamics simulation provides insights into the design of inhibitor systems with superior properties and also can be useful to find the corrosion inhibition mechanism [20, 21].

Benzothiazole and some of its derivatives have already been recommended as organic inhibitors for steel in hydrochloric acid. These compounds are heterocyclic molecules that are capable of

ACCEPTED MANUSCRIPT

binding to the surface of metal through N6GRQRUDWRPVDQGDOVREHOHFWURQV in aromatic cycles. In 1944, Ajmal *et al*. introduced a benzothiazole derivative as effective inhibitor for the corrosion of mild steel in 1 M HCl and 0.5 M H_2SO_4 and compared the behavior of inhibitor in this two acid solution [22]. Qurashi *et al*. later reported the 90% inhibition efficiency of four different substituted 2-amino benzothiazoles at concentration of 100-500ppm in 1 M HCl on mild steel using weight loss and potentiodynamic polarization methods and studied the effect of the functional groups, attached to the aromatic ring, on the corrosion inhibition [23]. N. S. Patel *et al*. in 2014 published a paper on the inhibitive effect of three different 2-amino benzothiazole derivatives using similar methods and experimental conditions, but obtained some results that are at odds with Qurashi's studies [3]. Khaled studied inhibition behavior of benzothiazole as an Indol derivative by electrochemical frequency modulation (EFM) method for corrosion of pure Iron in 1 M HCl to introduced EFM as a tool for online corrosion monitoring. They use theoretical techniques (quantum chemical calculation and MD simulation) but did not investigated any mechanism of corrosion inhibition and related adsorption process [24]. A. P. Samide *et al*. reported inhibition efficiency around 80% for 2-(cyclohexylaminomercapto) benzothiazole (4×10^{-4}M) in 1 M HCl on carbon steel. They proposed that the corrosion inhibition is adsorptive but did not investigated the mechanism of adsorption [25]. Popova *et al*. reported the results of several investigations on inhibitive effectiveness of benzothiazoles and cationic benzothiazolic quaternary ammonium bromides as inhibitors of mild steel in 1 M HCl. They used basic electrochemical methods to rationalize the influences of the structure of organic molecules on the inhibition efficiency and type of adsorption [26]. Markhali *et al*. investigated the inhibition behavior of benzothiazole and benzotriazole for corrosion of stainless steel in 1 M HCl by electrochemical noise measurement and showed that benzothiazole is more efficient as compared to benzotriazole

ACCEPTED MANUSCRIPT

[27]. Zhiyoung Hu *et al* reported the preparation of two benzothiazole derivatives with surface active properties as corrosion inhibitors for carbon steel in 1M HCl solution. Although, the synthesis procedure is a multistep and time consuming process with relatively low yield [28]. Though these investigations are valuable from experimental point of view, there are a few reports on theoretical and quantum chemical investigations and molecular dynamic simulation for understanding inhibition mechanism of benzothiazole derivatives.

Robust synthesis of 2-phenylbenzothiazole derivatives with short reaction time and rapid isolation of the products in high yield [29] and the existence of diverse functional groups in their structures make them excellent candidates as corrosion inhibitors. These characteristics provide a basis for investigating the effect of both physicochemical and electronic properties of these compounds on their inhibition behavior. In continuation of our work on the green synthesis and application of benzothiazole based ligands [29, 30], here in we report the detailed investigation on the inhibition behavior of three 2-phenylbenzothiazole derivatives on mild steel in hydrochloric acid solution using weight loss, electrochemical impedance spectroscopy, potentiodynamic polarization methods, and SEM surface analysis. Quantum chemical calculations based on density function theory (DFT) and MD simulation were further applied to discuss the effects of both physicochemical and electronic properties on their inhibition behavior by modelling of corrosion system and adsorption process.

2. Experimental

2.1. Preparation of the working electrode

Cylindrical mild steel specimens with composition (wt.%): C 0.180, Si 0.045, P 0.008, Al 0.010, Mn 0.618, S 0.021, Cu 0.179, Ni 0.100, Ti 0.006, Cr 0.078, V 0.003 and Fe balance were soldered to coated Cu-wires for electrical connections and then mounted in epoxy resin with an exposed

ACCEPTED MANUSCRIPT

area of 1 cm^2. Before each experiment, the surface of working electrode was mechanically abraded with emery papers down to 1200 grit and then rinsed with distilled water and acetone and derided in warm air flow.

2.2. Preparation of inhibitors and electrolytes

Three benzothiazole derivatives listed in Table 1 were synthesized according to the new procedure developed in our laboratory [29], by cyclocondensation of 2-aminothiophenol and three carboxylic acids under benign conditions using tetrabutylammonium bromide(TBAB) as the reaction medium and triphenyl phosphate as the catalyst. The corrosive solution (1 M HCl) was prepared from the reagent grade 37% HCl (MERCK, Art. 317) and deionized water. Solutions of the inhibitors in 1 M HCl were prepared with different concentrations (10, 20, 30. 40 and 50 ppm by weight).

2.3. Electrochemical measurements

Electrochemical measurements were carried out using a computer-controlled AMETEK potentiostat/galvanostat (model PARSTAT 2273) in a corrosion cell kit with a three electrode configuration. Mild steel, platinum and saturated calomel electrode (SCE) were employed as working electrode (WE), counter electrode and reference electrode, respectively. The surface of as-prepared WE was exposed to 250 ml electrolyte solution of 1 M HCl with and without inhibitors. First, the WE was immersed in the electrolyte solution for 1 h to establish a steady state open circuit potential (OCP). EIS measurements were then performed at OCP in a frequency range from 100 kHz to 10 mHz with a signal amplitude perturbation of 10 mV peak to peak. The polarization measurements were performed immediately after EIS measurements in the same corrosion cell containing the same electrode and test solution with a scan rate of 1 mV s^{-1} commencing from í 250 mV with respect to OCP to +250 mV. Corrosion current density values were obtained by Tafel extrapolation method. The experiments were performed in quiescent

ACCEPTED MANUSCRIPT

condition while the temperature was maintained constant (within ±1 ⁞C) using a water bath. The average values of three replicates obtained for each test are reported.

2.4. Weight loss measurements

Disk shape mild steel specimens of 38 mm diameter and 3 mm thickness with a hole of 8 mm diameter were prepared according to the ASTM standard [31], and were abraded with 80 grit emery paper, washed with distilled water, degreased with acetone, dried and kept in a desiccator. After weighing accurately, with sensitivity of ±0.1 mg, the specimens were immersed in a 500 mL glass cells containing 1 M HCl solution with and without various concentrations of inhibitors for 16 h. To clean the specimens after the test and remove all corrosion products from specimens with a minimum removal of sound metal, the specimens were taken out and rinsed thoroughly with distilled water and acetone, dried and weighted accurately again. In the present study, the average values of three replicates are reported.

2.5. Quantum chemical studies

Optimization of molecular structure was performed using the standard Gaussian 09 software package [32], Theoretical calculations were carried out using DFT at B3LYP functional with 6-311^{++}G(d,p) basis set for all atoms. Key parameters such as energies of LUMO (E_{LUMO}) and HOMO (E_{HOMO}), energy gap (' E) between LUMO and HOMO, dipole moment (μ) and the QXPEHUIWUDQVIHUUHGHOHFWURQIR Figure 1 benzothiazole derivatives were also determined.

2.6. Molecular dynamics (MD) simulation

MD simulation studies were performed using Material Studio 6.0 software from Accelrys Inc. The MD simulations were carried out in a simulation box (2.86 nm × 4.05 nm × 5.89 nm) with periodic boundary conditions to model a representative part of the interface devoid of any arbitrary

ACCEPTED MANUSCRIPT

boundary effects. Fe (1 1 0) surface is the most densely packed and also the most stable [33, 34]. Therefore, the Fe (1 1 0) was first cleaved from pure Fe crystal and relaxed by minimizing its energy using molecular mechanics. The surface area of Fe (1 1 0) was then enlarged to fabricate an appropriate super cell, and a vacuum slab with zero thickness was subsequently built above the Fe (1 1 0) super cell. Meanwhile, since the concentration of hydrochloric acid solution was 1 mol L^{-1}, and the corresponding proportion of water molecules to hydrogen chloride was 500/9, the adsorption system was included 491 H_2O, 9 H_3O^+, 9 Cl^- and 1 benzothiazole derivative. The system was constructed using the Amorphous Cell Program. Finally, the corrosion system, produced by placing the Amorphous Cell on Fe (1 1 0) super cell, was built by Layer Builder. Furthermore, eight layers of the ten layers near the bottom of supercell were kept fixed.

The MD simulations were performed by the COMPASS (condensed-phase optimized molecular potentials for atomistic simulation studies) force field under NVT ensemble (i.e. canonical ensemble) at 298 K (controlled by the Andersen thermostat) with a time step of 0.1 fs and a simulation time of 500 ps.

2.7. Surface morphological studies

After 16 h immersion in 1 M HCl solution with and without inhibitor, the corroded samples were washed with deionized water, dried and coated by a film of ~ 50 nm gold using sputtering technique. Surface morphology of the samples was then studied using a PHILIPS scanning electron microscope (SEM, model XL30)

3. Results and discussion

3.1. Potentiodynamic polarization measurements

Fig. 1a-c shows the representative potentiodynamic polarization curves of mild steel in 1 M HCl in the absence and presence of different concentrations of inhibitors at 25 ◦C. The values of

ACCEPTED MANUSCRIPT

related electrochemical parameters such as corrosion potential (E_{corr}), cathodic and anodic Tafel VORSHV DQG a), corrosion current density (i_{corr}) and inhibition efficiency (p %) were calculated from the related polarization curves and are given in Table 2. The surface coverage (P) and the p% were calculated from polarization readings according to equations 1 and 2, respectively [14, 35]:

$$\theta_p = \frac{i^{o}_{corr} - i_{corr}}{i^{o}_{corr}} \quad (1)$$

$$_p\% = \theta \times 100 \quad (2)$$

where i^{o}_{corr} and i_{corr} are the corrosion current densities under uninhibited and inhibited conditions, respectively. Corrosion current densities were extracted by Tafel extrapolating the cathodic and anodic branches of potentiodynamic polarization curves to cross at the front of the corresponding corrosion potential (E_{corr}). From Figure 1 and Table 2, it is clear that the addition of each compound causes a remarkable decrease in corrosion current density (i_{corr}). The decrease in the corrosion current densiWLHV at all inhibitor concentrations is in the order of **3** > **1** > **2**. It should be remarked that the anodic and cathodic Tafel slopes and also the values of E_{corr} remains almost constant by adding different concentration of the benzothiazole derivatives. This indicates that the benzothiazole derivatives are mixed type inhibitors and DFW DV ÐGVRUSWLYH LQKLELWRUV DQG G modify the reaction mechanism of corrosion process [36]. It is well known that the adsorptive inhibitors hinder the release of hydrogen gas on the metal surface and/or reduce the dissolution rate of metal into the aggressive solution by blocking the active sites on steel surface or even can mechanically screen the covered part of the electrode and therefore protect it from the action of corrosion medium [35, 37, 38]. In this way, the inhibition efficiency (p %) is expected to increase by increasing the corrosion inhibitor concentration, as evident from Table 2.

ACCEPTED MANUSCRIPT

3.2. Electrochemical impedance spectroscopy measurements

Prior to each test, the WE was immersed into the test solution for 1 h to attain the steady potential. Fig. 1 reveals the plots of open circuit potential (E_{OCP}) vs. immersion time (t) of mild steel in 1 M HCl solution at 25 ˚C in the absence and presence of inhibitor. It is clear that E_{OCP} remains almost constant after 1 h of immersion, which is indicative of the steady state.

The experimental impedance results of mild steel in 1 M HCl with and without inhibitors at OCP are displayed in Figs. 3-5. It is clear that the impedance response of mild steel is significantly changed after addition of benzothiazole derivatives and the diameter of the semi-circle increases in order of **3** > **1** > **2**. The complex plane plot (Nyquist) obtained in the absence and presence of inhibitors shows one capacitive loop at high frequency region and an inductive behavior at very low frequencies. The capacitive loop is attributed to the charge transfer resistance parallel to double-layer capacitance. The inductive behavior which appeared as a loop in most cases could be attributed to the relaxation process obtained by adsorption intermediate products such as $(FeCl^{-})_{ads}$ in the absence of inhibitor and $(FeCl^{-}Inh^{+})_{ads}$ in the presence of inhibitor [35, 39, 40]. The observation of depressed capacitive loop in the Nyquist plot of the inhibitors is presumably due to fast absorption of the aforementioned intermediate products [41, 42]. The deviation from ideal semicircle is mostly attributed to the frequency dispersion (depression effect) [12, 43].

In order to determine the impedance parameters from the experimental results, the data were fitted to the electrical equivalent circuit using the Zsimpwin software. Fig. 6 represents the electrical equivalent circuit in the absence and presence of inhibitors. Excellent fit results (with chi-squared less than 4×10^{-3}) were obtained using these circuits. In the equivalent circuit, R_s is the uncompensated solution resistance, R_{ct} refers to the charge-transfer resistance, Q is the constant phase element (CPE), L is the inductance, and R_L represent inductance resistor. The calculated

ACCEPTED MANUSCRIPT

impedance parameters derived from the complex plane plots are given in Table 3. In this case, due to the depression resulted by surface heterogeneity at a micro- or nano-level, such as the surface roughness/porosity, adsorption or diffusion, an acceptable fit could be obtained only if a CPE is used instead of capacitance in the equivalent circuit models [44-47]. The impedance function of CPE has the following form [12, 48, 49]:

$$Z_{CPE} \quad \frac{1}{Y_o \quad j \; Z^{n}} \qquad (3)$$

where Y_o and n are the magnitude of the CPE and the phase shift, respectively, which specifies the surface inhomogeneity, & LV WKH DQJXODU IUHTXHQF\IRU ZKLFK LPDJLQDU\SDUW RI WKH LPS reaches its maximum (equation 4);

$$Z \quad \frac{1}{R_{ct}Y_{o}\,\copyright}^{\frac{1}{n}} \qquad (4)$$

The inhibition efficiency ($_{Imp}$ %) are calculated using the following equation:

$$K_{Imp}\% \quad \frac{R_{ct} \quad R_{ct}^{o}}{R_{ct}} \quad 100 \qquad (5)$$

where $R^{\bullet}_{ct}$ and R_{ct} represent the charge transfer resistance values in the absence and presence of inhibitor, respectively.

As evident from Table 3, the values of Q (CPE of electrical double layer) has decreased and charge-transfer resistance has increased with increasing the inhibitors concentration. This may be attributed to the decrease in local dielectric constant and/or to the increase in the thickness of the electrical double layer. The decrease in the Q values is presumably due to the gradual replacement of water molecules and other ions originally adsorbed on the surface by the adsorbed inhibitor molecules. These results suggest that the benzothiazole derivatives act just via adsorption at the

ACCEPTED MANUSCRIPT

metal/solution interface (as adsorptive inhibitors). It is therefore reasonable to assume that the increase in polarization resistance is related directly to the adsorption of inhibitor molecules at metal/solution interface [4, 35]. The dissolution mechanism could be predicted by the values of phase shift (n) as an indicator. It is clear that, no significant change in the value of n is observed after addition of various concentrations of inhibitors (Table 3). The almost invariable values of n indicates that the charge transfer process controls the dissolution mechanism in both the absence and presence of various concentrations of benzothiazole derivatives [40]. The aforementioned results indicate that the EIS and potentiodynamic polarization measurements data correlate well with each other.

3.3. Weight loss measurements

The corrosion rates (C_{RW}) of mild steel in 1 M HCl in the absence and presence of various concentrations of the inhibitors were measured using the mass loss values after 16 h of immersion at 25 °C. The corrosion rate in millimeters per year (mm y^{-1}) was calculated from equation 6 [31]:

$$C_{Rw} \quad \frac{K \quad W}{A \quad t \quad \rho} \qquad (6)$$

where K is a constant equal to 8.76×10^4, t is the time of exposure in hours, W is the mass loss in gram, ρ the density in g cm^{-3} which is 7.86 g cm^{-3} for carbon steel according to ASTM G1-03 [50], and *A* is the surface area in cm^2 which is calculated from equation 7 [31]:

$$A \quad \frac{\pi}{2} D^2 \quad d^2 \quad l \quad D \quad l\pi d \qquad (7)$$

In this equation, *l* and *D* are the thickness and diameter of specimen, respectively, and *d* is the diameter of the hole for holding. The inhibition efficiency (K_W%) was also calculated according to

ACCEPTED MANUSCRIPT

equation 8:

$$K_W\% \quad \frac{C_{RW}^{o} \quad C_{RW}^{i}}{C_{RW}^{o}} \quad 100 \qquad (8)$$

where C_{RW}^{o} and C_{RW}^{i} are the corrosion rate of mild steel in the absence and presence of benzothiazole inhibitors, respectively. The results are given in Table 4. The values in Table 4 show that by increasing the concentration of benzothiazole derivatives, the corrosion rates of mild steel decrease (Fig.7), and the inhibition efficiencies ($K_W\%$) increase. This result suggests that more inhibitor molecules are adsorbed onto the surface of mild steel by increasing the inhibitor concentration, leading to the blocking of more corrosion active sites. The weight loss measurements indicate that the inhibition efficiency of inhibitors at the same concentration follows the order of **3** > **1** > **2**, and support the results obtained by electrochemical measurements (potentiodynamic and EIS).

Considering the inhibition efficiency of the three benzothiazole derivatives studied in this research, it is noticeable that the inhibition efficiency for compound **3** is more than 95% at very low concentration of this inhibitor (up to 50 ppm (by weight) § $^{-4}$ M) and is a more effective inhibitor for mild steel in acidic solution as compared to those reported in the literature for related compounds [4, 6, 18, 20, 21, 23, 35].

3.4. Adsorption isotherms

Since the first step in corrosion inhibition of metals and alloys is the adsorption of organic inhibitor molecules at the metal/solution interface, the efficiency of benzothiazole derivatives as a successful corrosion inhibitor mainly depends on their adsorption ability on the metal surface. Adsorption of inhibitor molecules from aqueous solutions is a quasi-substitution process, between

ACCEPTED MANUSCRIPT

the organic compounds in the aqueous phase ($Org_{(sol)}$) and water molecules at the electrode surface ($H_2O_{(ads)}$), because metal surface in aqueous solution is always covered with adsorbed water dipoles [4, 11, 35]:

$$Org_{(sol)} + xH_2O_{(ads)} \; / \; Org_{(ads)} + xH_2O_{(sol)} \qquad (9)$$

where $Org_{(ads)}$ and $H_2O_{(sol)}$ are the organic specie adsorbed on the metallic surface and the water molecule in solution, respectively, and x is the size ratio, that is, the number of water molecules replaced by one organic inhibitor. In order to obtain the isotherm, the values of surface coverage ( ) corresponding to the different inhibitors concentrations (C) (in mM) were used. For this purpose, the values of were calculated using the potentiodynamic polarization measurements according to the Eq. 1. In the present study, the experimental data fit well to the Langmuir adsorption isotherm as presented in Fig. 8a±c, and obtained from the following equation [10, 46, 51]:

$$\frac{C}{\theta} \quad \frac{1}{K_{ads}} \quad C \qquad (10)$$

where K_{ads} is the equilibrium constant for the adsorption±desorption process that can be calculated from the intercepts of the straight line on the C/D [illegible] K_{ads} values for the benzothiazole derivatives are given in Table 5. The higher magnitudes of K_{ads} reflect the higher adsorption ability of these benzothiazole derivatives on mild steel surface [28]. Moreover, relatively high inhibition efficiencies are obtained at low concentrations of these inhibitors.

A fitted straight line in Figs. 8a-c with slopes close to 1 suggests that the adsorption of these inhibitors on the mild steel surface conforms to the Langmuir adsorption isotherm and the adsorbed inhibitor molecules form a monolayer on mild steel surface with no interaction among them [11, 52].

ACCEPTED MANUSCRIPT

The standard free energy of the inhibitor adsorption (ΔG°_{ads}) can be calculated, using K_{ads}, by the equation 11 [4, 44]:

$$\Delta G^{o}_{ads} \quad RT \ln(55.5K_{ads}) \qquad (11)$$

where R is the universal gas constant, T is the absolute temperature and the constant value of 55.5 is the molar concentration of water in mol $dm^{\pm 3}$ in the solution. It is clear that the effectiveness of corrosion inhibition increases with the increase in K_{ads} and higher negative values of ΔG°_{ads}. The YDOXHV RI ΔG°_{ads} obtained in the present work are in the range of ±31.87 to ±40.8 kJ.$mol^{\pm 1}$ (Table 5). This indicates that the adsorption of the **1**, and **2** benzothiazoles on mild steel surface is neither merely SKYVLVRUSWLRQ (ΔG°_{ads} ~ íN-PRO $^{\pm 1}$ or less negative) nor merely chemisorption (ΔG°_{ads} ~ ±40 kJ $mol^{\pm 1}$ or more negative) [53-55], but obeys a comprehensive adsorption (both physisorption and chemisorption). However, it seems that the adsorption of **3** is more chemisorption as compared to **1** and **2**.

3.5. Quantum chemical calculations

To study the effect of electronic properties and molecular structure on inhibition efficiency of the three benzothiazole compounds and to rationalize the experimental data obtained from electrochemical readings and weight loss measurements, quantum chemical calculation has been applied. The geometry of three benzothiazole compounds **1**, **2**, and **3** obtained from the B3LYP/6-311G** method and the frontier molecular orbital density distributions (HOMO and LUMO) are shown in Fig. 9. The quantum chemical parameters, E_{HOMO}, E_{LUMO} (ΔE_{L-H} (energy gap between LUMO and HOMO) and μ (dipole moment) that directly influence electronic interaction between inhibitor molecule and metal surface have been calculated and are listed in Table 6.

TKH +202 DQG /802 HQHUJLHV DQG (ΔE_{L-H} are correlated with inhibition efficiency [12, 56, 57]. A higher value of E_{HOMO} leads to a stronger chemisorption and higher inhibition behavior for

ACCEPTED MANUSCRIPT

metal. Moreover, the ORZHU ûL-H (E_{LUMO} - E_{HOMO}) can cause stronger chemisorption of the inhibitor molecule on metal surface [12, 56-59].

The values of E_{HOMO} of the three benzothiazole derivatives (Table 6) show an increase in the order of **1** < **2** < **3**, and E_{LUMO} DQG ûL-H show a decrease in the order of **1** > **2** > **3**, which predict that benzothiazole **3** should be chemisorbed more effectively and had a better performance in comparison to **1** and **2**. This is in agreement with the experimental results and is also accord with WKH UHVXOWV REWDLQHG IURP WKH QXPEHU RI WUDQVIHUUHG HOHFWURQ ûN FDOFXOD quantum chemical method using equation 12 [11, 12, 56]:

$$N' \quad \frac{_{\mathrm{Fe}} \quad F_{\mathrm{Inh}}}{2 \quad _{\mathrm{Fe}} \quad J_{\mathrm{Inh}}} \qquad (12)$$

where $\$_{Fe}$ and $\$_{Inh}$ are the absolute electronegativity of iron and inhibitor, and $_{Fe}$ and $_{Inh}$ are the absolute hardness of iron and the inhibitor respectively. These terms are related to electron affinity (*A*) and ionization potential (*I*) as presented in equations 13 and 14:

$$F \quad \frac{I \quad A}{2} \qquad (13)$$

$$J \quad \frac{I \quad A}{2} \qquad (14)$$

ZKHUH DFFRUGLQJ WR .RRSDQ¶V WKHRUHP WKH *I* and *A* are related to the frontier orbital energies according to the equations 15 and 16 [12, 56]:

$$I \qquad E_{\mathrm{HOMO}} \qquad (15)$$

$$A \qquad E_{\mathrm{LOMO}} \qquad (16)$$

The YDOXHVRI$QGIRUEHQ]RWKLD]ROHFRPSRXQGV **1**, **2** and **3** were calculated using the values of *I* and *A* REWDLQHGIURPTXDQWXPFKHPLFDOFDOFXODWLRQV7KHWKHRUHWLFDO$YDOX ±1 and value of 0 eV mol$^{\pm1}$ for iron was used from the literature [11, 56]. According to Lukovits

ACCEPTED MANUSCRIPT

[60], LI WKHFKHPLVRUSWLRQDQGLQKLELWLRQHIILFLHQF WHQGHQF LQFUHDVHVZLWKW in the electron-donating ability at the metal surface. This shows that as the strength of the iron- inhiELWRU ERQG LQFUHDVHV DV D UHVXOW RI LQFUHDVLQJ WKH GHJUHH RI FRUURVLRQ L FKHPLVRUSWLRQ LV LQFUHDVHG 7KH FDOFXODWHG YDOXHV IRU WKH EHQ]RWKLD]ROHG order of **1** < **2** < **3**, (0.6576, 0.7017, 0.9042 for **1**, **2**, and **3**, respectively) which again shows that the benzothiazole **3** chemisorbs more strongly. It is well known that the chemisorption of inhibitor molecules provides higher corrosion inhibition when compared to physisorption. According to the experimental data, the corrosion inhibition efficiency of benzothiazole **3** should be the highest. This confirms that this derivative is adsorbed mainly chemically. However, for the benzothiazole **1** and **2**, the calculated quantum chemical parameters show no direct correlation with their inhibition performance obtained from the experiments. As mentioned before, the corrosion inhibition of these two derivatives is a complicated process involving both chemical and physical adsorptions [21]. It is evident from the molecular structures of benzothiazoles **1** and **2** (Table 1) that benzothiazole **2** can be protonated more readily than benzothiazole **1**, due to the presence of two hydroxyl group in its structure, and thus, stronger electrostatic interaction (or stronger physisorption) is expected for benzothiazole **2**. Nevertheless, in spite of the stronger physisorption predicted for this molecule, it is a less effective inhibitor than benzothiazole **1**. This contradiction is presumably due to the difference in the structural characteristics of these two inhibitors which affects the configuration of the adsorbed inhibitor molecule on the metal surface as discussed in the following section.

ACCEPTED MANUSCRIPT

3.6. Molecular dynamics (MD) simulation

Recently, MD simulations have been employed to investigate the adsorption behavior of the inhibitor molecule on the metallic surfaces [17, 20, 34, 61], MD simulation can reasonably predict the most favorable configuration of the adsorbed inhibitor molecule on the metal surface at molecular level, and give some insights into the difference in inhibitive performance by obtaining the values of adsorption energy ($E_{adsorption}$) and binding energy $E_{binding}$ between the organic inhibitor and metal surface. To study the extent of the interaction (including both physical and chemical) of the corrosion inhibitors absorbed on the surface, the values of $E_{adsorption}$ and $E_{binding}$ of the three inhibitor molecules **1**, **2**, **3** on the Fe (1 1 0) surface were calculated according to the equations 17 and 18 [33]:

$$E_{adsorption} \quad E_{total} \quad (E_{surface\ \ solution} \quad E_{inhibitor\ \ solution}) \quad E_{solution} \tag{17}$$

$$E_{binding} \quad E_{adsorption} \tag{18}$$

Herein, the total energy of the simulation system, E_{total}, includes the iron crystal together with the adsorbed inhibitor molecule on the iron surface and the solution; $E_{surface+solution}$ is the total energy of the system without the inhibitor; $E_{inhibitor+solution}$ is the total energy of the system without the iron crystal; and the total energy of the solution is designated as $E_{solution}$.

Thus, for a better insightfulness on the adsorption behavior of all three selected inhibitors, MD simulation was performed and the values of $E_{adsorption}$ and $E_{binding}$ between the inhibitor and Fe (1 1 0) surface were obtained under equilibrium conditions according to the Eq. (17) and (18), respectively. The top and side views of the equilibrium configurations of the inhibitor molecules over the Fe (1 1 0) surface are depicted in Fig. 10. It is evident that the inhibitor molecules are adsorbed on the Fe (1 1 0) surface with an almost flat orientation. This parallel or flat disposition on the iron surface can be attributed to the nearly equal distribution of HOMO and LUMO

ACCEPTED MANUSCRIPT

densities on the whole molecule. Therefore, the whole inhibitor molecule can donate electrons to the unoccupied orbitals of the iron surface to form stable coordination bonds, and also accept electrons from the d-orbitals of iron through back-bonding [41].

Generally, the bond distance shorter than 3.5 ˚A indicates that there is a strong chemical bond formation between the atoms and longer bond lengths specifies that the interactions between the atoms are of van der Waals type [17, 62]. The calculated shortest bond distances between the closest hetero atoms of the inhibitors **1**, **2**, **3** and Fe (1 1 0) surface are as follows: **1**-Fe interaction: (Fe-N = 3.144 ˚A, Fe-S = 3.117 ˚A), **2**-Fe interaction: (Fe-N=3.379 ˚A, Fe-S=3.216 ˚A), **3**-Fe interaction: (Fe-N=3.084 ˚A, Fe-S=3.038 ˚A). These values confirm that there is a chemical bond formation between the benzothiazole derivatives and Fe surface. However, longer bond distances indicate that there are also van der Waals interactions in the adsorption process of the inhibitors with Fe surface. It could be concluded that the benzothiazole **3** showing the lowest bond distance tends to have stronger chemical interaction with the steel surface as previously realized from quantum chemical calculation.

The calculated binding energies and interaction energies for the investigated systems are listed in Table 7. The high negative values of the interaction energy between benzothiazole derivatives and the iron surface implies that the interaction between inhibitor molecules and iron surface is spontaneous, strong and stable [34, 63]. Moreover, the interaction energies are in the order of: **3** (í 622.98 kJ mol^{-1}) < **1** (í 550.36 kJ mol^{-1}) < **2** (í 528.13 kJ mol^{-1}).

From the theoretical point of view, a higher value of $E_{binding}$ indicates that the adsorption system is more stable and the inhibitor molecule should exhibit higher inhibition efficiency. Thus, considering the calculated values of the interaction and binding energies, the stability of the adsorption systems and inhibition efficiency show the order of **3** > **1**> **2**.

ACCEPTED MANUSCRIPT

The results obtained from MD simulation are in good agreement with the experimentally determined inhibition efficiencies, and confirms that this method is a powerful tool in the investigation of the corrosion inhibitors behavior, especially when the stability of inhibitor adsorption on metal surface is a determining factor. MD also gives useful information at the molecular level about the systems under investigation.

3.7. SEM studies

SEM micrographs of the mild steel surface after 16 h immersion at 25 ◦C in 1 M HCl in the absence and presence of 50 ppm by wieght of the inhibitors are displayed in Fig. 11. As evident from Fig. 11a, the mild steel surface is strongly attacked in the absence of inhibitors due to the intensive metal dissolution, leading to highly porous surface with large and deep holes. In contrast, in the presence of the benzothiazole derivatives (Figs. 11b-d), the appearance of the steel surface is significantly improved, with almost no pores except for the polishing lines, that are observed on the micrograph. The observation of polishing lines in the presence of inhibitors **3** and **1** (Fig. 11b and Fig. 11d) indicates their higher inhibition performances. These results are in good agreement with the electrochemical experiments and weight loss measurements, wherein inhibition performance of **2** is lower than **1** and **3**, while **3** has the best performance.

3.8. Chemical structure and mechanism of corrosion inhibition

Adsorption is a rapid process which covers the metal surface or just blocks the active sites of metal surface from aggressive media [11]. The thermodynamic parameters of adsorption obtained in this study show that the inhibitors **1** and **2** are adsorbed on the mild steel surface through both physical

ACCEPTED MANUSCRIPT

and chemical mechanisms while inhibitor **3** is adsorbed mainly chemically. The surface charge of the metal can be defined by comparing the potential of zero charge (PZC) and corrosion potential. The PZC of steel can be considered zero due to the contact adsorption of Cl^- [64]. In this study, E_{corr} value of mild steel in 1 M HCl is í 482 mV vs. SCE (Table 2). Accordingly, the metal carries a negative surface charge, because E_{corr} í PZC <0. The benzothiazole molecules are expected to be protonated in strong acid solutions, and as a result, the protonated species can be adsorbed physically [35, 65]. In addition, the protonated benzothiazole molecules are also adsorbed onto the cathodic sites of the mild steel in competition with hydrogen ions, and reduce the rate of hydrogen evolution reaction [55, 66].

In chemisorption, the strong adsorption of molecules on a metal surface can be considered as an acid-base reaction in which the organic molecule acts as a base and donates electron to the metal, acting as an acid [67]. 7KHVWDELOLW\RIDGVRUSWLRQLVGHWHUPLQHGE\HDUVRQ+6%SULQ
From the variations in the positive oxidation state of metal, it can be predicted that metal atoms are at zero oxidation state and the surface of bulk metals will always be soft acids [67]. So, the adsorption of soft base molecule on metal surface is strong and soft base molecules behave more effective as an inhibitor.

To rationalize the inhibitory behavior of benzothiazoles used in this study, it is necessary at this point to evaluate the experimental and theoretical results and find how these results correlate with the chemical, structural, and electronic characteristics of these inhibitors. The benzothiazole derivatives studied in this work contain nitrogen, oxygen and sulfur hetero atoms in their structures (Table 1). The HOMO orbital in these molecules, as shown in Fig. 9, is mostly localized on the thiazole ring indicating that the free electron pairs are available for nucleophilic interaction with the metal surface, containing the reaction centers for chemisorption process. This makes the

ACCEPTED MANUSCRIPT

inhibitors capable of forming a co-RUGLQDWH ERQG ZLWK)H 7KH π-electron system from the aromatic rings and the HOMO density distributions on these parts of the molecule (Fig. 9) also PDNHV WKHP VXLWDEOH IRU LQWHUDFWLRQ ZLWK WKH PHWDO VXUIDFH 7KH π-system also allows back donation of metal d-HOHFWURQV WR WKH π* orbitals of the inhibitors [69]. The presence of sulfur in the VWUXFWXUH RI WKHVH LQKLELWRUV PDNH WKH FRRUGLQDWH LRQLF ERQG IRUPDWLRQ IURP WKH RYHUODS RI G electrons of Fe atom to 3d vacant orbitals of sulfur atom, possible [70, 71], and thus enhancing their adsorption on the metal surface. These features make the benzothiazole derivatives to be considered as powerful inhibitors.

The experimental results of the electrochemical measurements confirm that adding trace concentrations of these inhibitors (i.e. 50 ppm by weight) leads to upto 95% inhibition efficiency. The inhibition efficiency values in 1 M HCl follow the order of **3** > **1** > **2**. The quantum chemical results and the structural properties such as the presence of different substitutions in the benzothiazole moiety are used to explain different inhibition effectiveness. The presence of extra nitrogen hetero atom from dimethyl amine group at para position of the phenyl ring in **3** as well as the presence of two electron donating ±CH_3 groups, intensifies its chemisorption and leads to a KLJKHU LQKLELWLRQ HIILFLHQF\ 6WURQJ LQWHUDFWLRQ RI π-electrons with metal surface requires a so-called face-on orientation in which the aromatic ring is positioned parallel with the metal surface [11]. It is evident from the optimized geometry of benzothiazole derivatives (Fig. 9) that the structure of benzothiazole **3** LV FORVH WR SODQDU ZKLFK DOVR IDYRUV D VWURQJ π-LQWHUDFWLRQ RI π-electrons with metal surface. However, the benzothiazoles **1** and **2** show tilted structures. The presence of hydroxyl group at ortho position in **1** and **2** molecules render the phenyl ring away from the planarity resulting in less chemisorption and leads to lower inhibition efficiencies [11]. The higher inhibition efficiency of **1** relative to **2** (Tables 2 - 4) may be attributed to its higher

ACCEPTED MANUSCRIPT

tendency for physisorption. But, the presence of an extra hydroxyl group at the meta position of phenyl ring in **2** provides additional centers for protonation. Consequently, a stronger electrostatic interaction with metal (i.e. stronger physisorption) is expected for **2** as compared to **1**. If so, this should lead to a higher inhibition efficiency of **2**, being in odd with the experimental results. Alternatively, the difference between inhibition efficiency of **1** and **2** may be related to their chemisorption characteristics. Since, according to the quantum chemical calculations, there are no noticeable differences between the electronic properties of **1** and **2** (Table 6), the structural properties are presumably decisive in chemisorption and the inhibition behavior observed for benzothiazoles **1** and **2**. A key structural parameter that contributes to the spatial orientation of benzothiazole molecules is hydrogen bonding. **1** forms interamolecular H-bonding while **2** is involved in intermolecular H-bonding between the neighboring molecules. Interamolecular H-bond in **1** changes its tilted structure to almost planer leading to more favorable chemisorption [72]. However the structure of the layer formed by **2** on the metal surface becomes disordered due to the tilted structure and the intermolecular H-bond, and consequently, it cannot cover the metal surface quite efficiently [70]. Therefore, in the presence of **2**, more active sites on the metal are still exposed to HCl and as a result, lower inhibition efficiency is observed for inhibitor **2** relative to **1**. These results conform very well to the MD calculations.

4. Conclusion

The inhibition behavior of three benzothiazole derivatives **1**, **2** and **3** were investigated using weight loss, electrochemical methods, SEM surface analysis, quantum chemical calculations and MD simulation. The inhibition efficiencies of these benzothiazole derivatives on the corrosion of mild steel in 1 M HCl decrease in the order of **3** > **1** > **2** at all concentrations. The potentiodynamic polarization measurements showed that these organic compounds are mixed-type inhibitors and act

ACCEPTED MANUSCRIPT

as adsorptive inhibitors, so by increasing corrosion inhibitor concentration (up to 50 ppm by weight) the inhibition efficiency is increased. The electrochemical impedance spectroscopy indicated that the CPE of electrical double layer decreased and charge-transfer resistance increased with increasing the inhibitor concentration. These results also confirm that the benzothiazole derivatives act just via adsorption at the metal/solution interface. The stability of the values of phase shift (n) reveals that the charge transfer process controls the dissolution mechanism of mild steel in 1 M HCl solution in the absence and presence of various concentrations of benzothiazole derivatives. The experimental data fit well by Langmuir adsorption isotherm model, and the thermodynamic parameters obtained from adsorption isotherm confirm that these benzothiazole molecules are strongly adsorbed onto the mild steel surface and the adsorption is predominately chemisorption for **3**, but, comprehensive (both physisorption and chemisorption) for **1** and **2**. This result is related to the structure of benzothiazole **3** which is close to planar but the benzothiazoles **1** and **2** show tilted structures.

Quantum chemical calculation results predict that the benzothiazole **3** is the most effective inhibitor in preventing corrosion and conform to the experimental results obtained for **3**. However, the order of the experimental inhibition efficiencies of **1** and **2** are not in agreement with quantum chemical calculation results. This suggests that the corrosion inhibition of these compounds is a complicated process and the molecular electronic parameters are not sufficient to predict their relative chemisorption. It can safely be speculated that the difference in the inhibition efficiencies observed for **1** and **2** lies in the difference in their configuration on the metal surface. The layer formed by the molecules of **2** on the metal surface is disordered due to the tilted structure and the intermolecular H-bond leading to its lower inhibition efficiency. The configuration of molecules on metal surface was simulated using MD. The results reveal that the three benzothiazole

ACCEPTED MANUSCRIPT

derivatives are adsorbed onto the mild steel surface in a nearly flat manner with high negative $E_{binding}$ and the sequence is perfectly in accordance with the experimentally observed inhibition efficiencies. The inhibition behavior of the benzothiazoles used in this study was also confirmed by taking SEM micrographs of the surfaces exposed to the inhibited solution which was in good agreement with the electrochemical experiments and weight loss measurements.

Acknowledgments

Partial support of this work by the Research Council of the Isfahan University of Technology is gratefully acknowledged.

Reference

[1] S.A. El-Maksoud, The effect of organic compounds on the electrochemical behaviour of steel in acidic media. A review, Int. J. Electrochem. Sci. 3 (2008) 528-555.

[2] E. Gutiérrez, J.A. Rodríguez, J. Cruz-Borbolla, J.G. Alvarado-Rodríguez, P. Thangarasu, Development of a predictive model for corrosion inhibition of carbon steel by imidazole and benzimidazole derivatives, Corros. Sci.108 (2016) 23-35.

[3] N. Patel, P. Beranek, M. Nebyla, M. Pribyl, D. Snita, Inhibitive effects by some benzothiazole derivatives on mild steel corrosion in 1 N HCl, Int. J. Electrochem. Sci. 9 (2014) 3951-3960.

[4] R. Solmaz, Investigation of the inhibition effect of 5-((E)-4-phenylbuta-1, 3-dienylideneamino)-1, 3, 4-thiadiazole-2-thiol Schiff base on m ild steel corrosion in hydrochloric acid, Corros. Sci. 52 (2010) 3321-3330.

[5] A.P. Samide, I. Bibicu, Kinetics corrosion process of carbon steel in hydrochloric acid in

absence and presence of 2-(cyclohexylaminomercapto) benzothiazole, Surf. Interface Anal. 40 (2008) 944-952.

[6] M. Behpour, S. Ghoreishi, N. Mohammadi, N. Soltani, M. Salavati-Niasari, Investigation of some Schiff base compounds containing disulfide bond as HCl corrosion inhibitors for mild steel, Corros. Sci. 52 (2010) 4046-4057.

>@ 0)LQãJDU '. 0HUO $Q HOHFWURFKHPLFDO ORQJ-term immersion, and XPS study of 2-mercaptobenzothiazole as a copper corrosion inhibitor in chloride solution, Corros. Sci. 83 (2014) 164-175.

[8] A. Döner, R. Solmaz, M. ÖzcaQ*.DUGDú([SHULPHQWDODQGWKHRUHWLFDOVWXGLHVRIWK

as corrosion inhibitors for mild steel in sulphuric acid solution, Corros. Sci. 53 (2011) 2902-2913.

>@$<•FH%'0HUW*.DUGDú%<D]Õ(OHFWURFKHPLFDODQGTXDQWXPFKHPLFDOVWXGLH of 2-amino-4-methyl-thiazole as corrosion inhibitor for mild steel in HCl solution, Corros. Sci. 83 (2014) 310-316.

[10] S. Shahabi, P. Norouzi, M.R. Ganjali, Electrochemical and theoretical study of the inhibition effect of two synthesized thiosemicarbazide derivatives on carbon steel corrosion in hydrochloric acid solution, RSC Adv. 5 (2015) 20838-20847.

[11] I. Ahamad, R. Prasad, M. Quraishi, Experimental and quantum chemical characterization of the adsorption of some Schiff base compounds of phthaloyl thiocarbohydrazide on the mild steel in acid solutions, Mater. Chem. Phys. 124 (2010) 1155-1165.

[12] D. Daoud, T. Douadi, H. Hamani, S. Chafaa, M. Al-Noaimi, Corrosion inhibition of mild

ACCEPTED MANUSCRIPT

steel by two new S-heterocyclic compounds in 1 M HCl: experimental and computational study, Corros. Sci. 94 (2015) 21-37.

[13] S. Hejazi, S. Mohajernia, M. Moayed, A. Davoodi, M. Rahimizadeh, M. Momeni, A. Eslami, A. Shiri, A. Kosari, Electrochemical and quantum chemical study of Thiazolo-pyrimidine derivatives as corrosion inhibitors on mild steel in 1M H_2SO_4, J. Ind. Eng. Chem. 25 (2015) 112-121.

[14] H.M.A. El-Lateef, M.A. Abo-Riya, A.H. Tantawy, Empirical and quantum chemical studies on the corrosion inhibition performance of some novel synthesized cationic gemini surfactants on carbon steel pipelines in acid pickling processes, Corros. Sci. 108 (2016) 94-110.

[15] G. Gece, The use of quantum chemical methods in corrosion inhibitor studies, Corros. Sci. 50 (2008) 2981-2992.

[16] V. Torres, V. Rayol, M. Magalhães, G. ViaQD/$XLDU60DFKDGR+2URILQR('¶OLD Study of thioureas derivatives synthesized from a green route as corrosion inhibitors for mild steel in HCl solution, Corros. Sci. 79 (2014) 108-118.

[17] S.K. Saha, P. Banerjee, A theoretical approach to understand the inhibition mechanism of steel corrosion with two aminobenzonitrile inhibitors, RSC Adv. 5 (2015) 71120-71130.

[18] E.E. Ebenso, M.M. Kabanda, L.C. Murulana, A.K. Singh, S.K. Shukla, Electrochemical and quantum chemical investigation of some azine and thiazine dyes as potential corrosion inhibitors for mild steel in hydrochloric acid solution, Ind. Eng. Chem. Res. 51 (2012) 12940-12958.

[19] M. Quraishi, Electrochemical and theoretical investigation of triazole derivatives on corrosion

ACCEPTED MANUSCRIPT

inhibition behavior of copper in hydrochloric acid medium, Corros. Sci. 70 (2013) 161-169.

[20] S.K. Saha, A. Dutta, P. Ghosh, D. Sukul, P. Banerjee, Adsorption and corrosion inhibition effect of Schiff base molecules on the mild steel surface in 1 M HCl medium: a combined experimental and theoretical approach, Phys. Chem. Chem. Phys. 17 (2015) 5679-5690.

[21] S.K. Saha, A. Dutta, P. Ghosh, D. Sukul, P. Banerjee, Novel Schiff base molecules as efficient corrosion inhibitors for mild steel surface in 1 M HCl medium: Experimental and theoretical approach, Phys. Chem. Chem. Phys. 18 (2016) 17898-17911.

[22] M. Ajmal, A. Mideen, M. Quraishi, 2-Hydrazino-6-methyl-benzothiazole as an effective inhibitor for the corrosion of mild steel in acidic solutions, Corros. Sci. 36 (1994) 79-84.

[23] M. Quraishi, M.W. Khan, M. Ajmal, S. Muralidharan, S.V. Iyer, Influence of substituted benzothiazoles on corrosion in acid solution, J. Appl. Electrochem. 26 (1996) 1253-1258.

[24] K. Khaled, Application of electrochemical frequency modulation for monitoring corrosion and corrosion inhibition of iron by some indole derivatives in molar hydrochloric acid, Mater. Chem. Phys. 112 (2008) 290-300.

[25] A. Patru Samide, I. Bibicu, Kinetics corrosion process of carbon steel in hydrochloric acid in absence and presence of 2a(cyclohexylaminomercapto) benzothiazole, Surf. Interface Anal. 40 (2008) 944-952.

[26] A. Popova, M. Christov, A. Vasilev, Mono-and dicationic benzothiazolic quaternary ammonium bromides as mild steel corrosion inhibitors. Part II: Electrochemical impedance and polarisation resistance results, Corros. Sci. 53 (2011) 1770-1777.

ACCEPTED MANUSCRIPT

[27] B. Markhali, R. Naderi, M. Mahdavian, M. Sayebani, S. Arman, Electrochemical impedance spectroscopy and electrochemical noise measurements as tools to evaluate corrosion inhibition of azole compounds on stainless steel in acidic media, Corros. Sci. 75 (2013) 269-279.

[28] Z. Hu, Y. Meng, X. Ma, H. Zhu, J. Li, C. Li, D. Cao, Experimental and theoretical studies of benzothiazole derivatives as corrosion inhibitors for carbon steel in 1M HCl, Corros. Sci. 112 (2016) 563-575.

[29] S. Meghdadi, M. Amirnasr, P.C. Ford, A robust one-pot synthesis of benzothiazoles from carboxylic acids including examples with hydroxyl and amino substituents, Tetrahedron Lett. 53 (2012) 6950-6953.

[30] S. Meghdadi, M. Amirnasr, A. Mirhashemi, A. Amiri, Synthesis, characterization and X-ray crystal structure of copper (I) complexes of the 2-(2-quinolyl) benzothiazole ligand. Electrochemical and antibacterial studies, Polyhedron 97 (2015) 234-239.

[31] $670 6WDQGDUG 3UDFWLFHV IRU /DERUDWRU\,PPHUVLRQ &RUURVLRQ 7HVWLQJ RI Annual Book of ASTM Standards, G 31-72, Philadelphia, PA, (1990).

[32] M. Frisch, G. Trucks, H. Schlegel, G. Scuseria, M. Robb, J. Cheeseman, G. Scalmani, V. Barone, B. Mennucci, G. Petersson, Gaussian 09, revision A. 1, Gaussian Inc., Wallingford, CT, (2009).

[33] L. Li, X. Zhang, S. Gong, H. Zhao, Y. Bai, Q. Li, L. Ji, The discussion of descriptors for the QSAR model and molecular dynamics simulation of benzimidazole derivatives as corrosion inhibitors, Corros. Sci. 99 (2015) 76-88.

[34] I. Obot, N. Obi-Egbedi, E. Ebenso, A. Afolabi, E. Oguzie, Experimental, quantum chemical calculations, and molecular dynamic simulations insight into the corrosion inhibition properties of 2-(6-methylpyridin-2-yl) oxazolo [5, 4-f][1, 10] phenanthroline on mild steel, Res. Chem. Intermed. 39 (2013) 1927-1948.

[35] J. Aljourani, K. Raeissi, M. Golozar, Benzimidazole and its derivatives as corrosion inhibitors for mild steel in 1M HCl solution, Corros. Sci. 51 (2009) 1836-1843.

[36] M. Hegazy, A. Badawi, S.A. El Rehim, W. Kamel, Corrosion inhibition of carbon steel using novel N-(2-(2-mercaptoacetoxy) ethyl)-N, N-dimethyl dodecan-1-aminium bromide during acid pickling, Corros. Sci. 69 (2013) 110-122.

[37] F. Zhang, Y. Tang, Z. Cao, W. Jing, Z. Wu, Y. Chen, Performance and theoretical study on corrosion inhibition of 2-(4-pyridyl)-benzimidazole for mild steel in hydrochloric acid, Corros. Sci. 61 (2012) 1-9.

>@5<ÕGÕ]$QHOHFWURFKHPLFDODQGWKHRUHWLFDOHYDOXDWLRQRI4,6-diamino-2-pyrimidinethiol as a corrosion inhibitor for mild steel in HCl solutions, Corros. Sci. 90 (2015) 544-553.

>@ 5 6ROPD] * .DUGDú 0 &XOKD % <D]ÕFÕ 0 (UELO ,QYHVWLJDWLR n of adsorption and inhibitive effect of 2-mercaptothiazoline on corrosion of mild steel in hydrochloric acid media, Electrochim. Acta 53 (2008) 5941-5952.

>@ 0 g]FDQ) .DUDGD÷ 'HKUL ,QWHUIDFLDO EHKDYLRU RI FVWHLQH EHWZHHQ PLOG VWHH sulfuric acid as corrosion inhibitor, Acta Phys. Chim. Sin. 24 (2008) 1387-1392.

[41] S. Deng, X. Li, X. Xie, Hydroxymethyl urea and 1, 3-bis (hydroxymethyl) urea as corrosion

ACCEPTED MANUSCRIPT

inhibitors for steel in HCl solution, Corros. Sci. 80 (2014) 276-289.

[42] C.M. Goulart, A. Esteves-Souza, C.A. Martinez-Huitle, C.J.F. Rodrigues, M.A.M. Maciel, A. Echevarria, Experimental and theoretical evaluation of semicarbazones and thiosemicarbazones as organic corrosion inhibitors, Corros. Sci. 67 (2013) 281-291.

[43] D. Daoud, T. Douadi, S. Issaadi, S. Chafaa, Adsorption and corrosion inhibition of new synthesized thiophene Schiff base on mild steel X52 in HCl and H_2SO_4 solutions, Corros. Sci. 79 (2014) 50-58.

>@%'0HUW$<FH*.DUGD%<D]ÊÕQKLELWLRQHIIHFWRI -amino-4-methylpyridine on mild steel corrosion: Experimental and theoretical investigation, Corros. Sci.85 (2014) 287-295.

[45] T.H. Muster, H. Sullivan, D. Lau, D.L.J. Alexander, N. Sherman, S.J. Garcia, T.G. Harvey, T.A. Markley, A.E. Hughes, P.A. Corrigan, A.M. Glenn, P.A. White, S.G. Hardin, J. Mardel, J.M.C. Mol, A combinatorial matrix of rare earth chloride mixtures as corrosion inhibitors of AA2024-T3: Optimisation using potentiodynamic polarisation and EIS, Electrochim. Acta 67 (2012) 95-103.

[46] M. Chevalier, F. Robert, N. Amusant, M. Traisnel, C. Roos, M. Lebrini, Enhanced corrosion resistance of mild steel in 1 M hydrochloric acid solution by alkaloids extract from Aniba rosaeodora plant: Electrochemical, phytochemical and XPS studies, Electrochim. Acta 131 (2014) 96-105.

[47] K. Boumhara, M. Tabyaoui, C. Jama, F. Bentiss, Artemisia Mesatlantica essential oil as green inhibitor for carbon steel corrosion in 1M HCl solution: Electrochemical and XPS investigations, J. Ind. Eng. Chem. 29 (2015) 146-155.

ACCEPTED MANUSCRIPT

[48] B. Qian, J. Wang, M. Zheng, B. Hou, Synergistic effect of polyaspartic acid and iodide ion on corrosion inhibition of mild steel in H_2SO_4, Corros. Sci. 75 (2013) 184-192.

[49] Z. Cao, Y. Tang, H. Cang, J. Xu, G. Lu, W. Jing, Novel benzimidazole derivatives as corrosion inhibitors of mild steel in the acidic media. Part II: Theoretical studies, Corros. Sci. 83 (2014) 292-298.

[50] ASTM, "Standard practice for preparing, cleaning, and evaluating corrosion test specimens", Annual Book of ASTM Standards, G1-03 (2011).

[51] X. Zheng, S. Zhang, W. Li, L. Yin, J. He, J. Wu, Investigation of 1-butyl-3-methyl-1H-benzimidazolium iodide as inhibitor for mild steel in sulfuric acid solution, Corros. Sci. 80 (2014) 383-392.

[52] A. Badiea, K. Mohana, Effect of temperature and fluid velocity on corrosion mechanism of low carbon steel in presence of 2-hydrazino-4, 7-dimethylbenzothiazole in industrial water medium, Corros. Sci. 51 (2009) 2231-2241.

[53] M. Pavithra, T. Venkatesha, M.P. Kumar, H. Tondan, Inhibition of mild steel corrosion by Rabeprazole sulfide, Corros. Sci. 60 (2012) 104-111.

>@ , -HYUHPRYLü 0 6LQJHU 6 1HãLü 9 0LãNRYLü -6WDQNRYLüQKLELWLRQ SURSHUWLHV RI V assembled corrosion inhibitor talloil diethylenetriamine imidazoline for mild steel corrosion in chloride solution saturated with carbon dioxide, Corros. Sci. 77 (2013) 265-272.

[55] R. Solmaz, Investigation of adsorption and corrosion inhibition of mild steel in hydrochloric acid solution by 5-(4-Dimethylaminobenzylidene) rhodanine, Corros. Sci. 79 (2014) 169-176.

ACCEPTED MANUSCRIPT

[56] V. Sastri, J. Perumareddi, Molecular orbital theoretical studies of some organic corrosion inhibitors, Corrosion 53 (1997) 617-622.

[57] I. Obot, D. Macdonald, Z. Gasem, Density functional theory (DFT) as a powerful tool for designing new organic corrosion inhibitors. Part 1: an overview, Corros. Sci. 99 (2015) 1-30.

[58] L.M. Rodríguez-Valdez, W. Villamisar, M. Casales, J. Gonzalez-Rodriguez, A. Martínez-Villafañe, L. Martinez, D. Glossman-Mitnik, Computational simulations of the molecular structure and corrosion properties of amidoethyl, aminoethyl and hydroxyethyl imidazolines inhibitors, Corros. Sci. 48 (2006) 4053-4064.

[59] A. Fouda, A. Ellithy, Inhibition effect of 4-phenylthiazole derivatives on corrosion of 304L stainless steel in HCl solution, Corros. Sci. 51 (2009) 868-875.

[60] I. Lukovits, E. Kalman, F. Zucchi, Corrosion inhibitors-correlation between electronic structure and efficiency, Corrosion 57 (2001) 3-8.

[61] I. Obot, Z. Gasem, Theoretical evaluation of corrosion inhibition performance of some pyrazine derivatives, Corros. Sci. 83 (2014) 359-366.

[62] S. Umoren, I. Obot, A. Madhankumar, Z. Gasem, Effect of degree of hydrolysis of polyvinyl alcohol on the corrosion inhibition of steel: theoretical and experimental studies, J. Adhes. Sci. Technol. 29 (2015) 271-295.

[63] J. Zhou, S. Chen, L. Zhang, Y. Feng, H. Zhai, Studies of protection of self-assembled films by 2-mercapto-5-methyl-1, 3, 4-thiadiazole on iron surface in 0.1M H_2SO_4 solutions, J. Electroanal. Chem. 612 (2008) 257-268.

ACCEPTED MANUSCRIPT

[64] V. Sastri, Corrosion inhibitors: principles and applications, 1998.

[65] E.E. Oguzie, Evaluation of the inhibitive effect of some plant extracts on the acid corrosion of mild steel, Corros. Sci. 50 (2008) 2993-2998.

[66] Q.B. Zhang, Y.X. Hua, Corrosion inhibition of mild steel by alkylimidazolium ionic liquids in hydrochloric acid, Electrochim. Acta 54 (2009) 1881-1887.

[67] R.G. Pearson, Hard and soft acids and bases, J. Am. Chem. Soc. 85 (1963) 3533-3539.

[68] S. Martinez, Inhibitory mechanism of mimosa tannin using molecular modeling and substitutional adsorption isotherms, Mater. Chem. Phys. 77 (2003) 97-102.

[69] M. Hosseini, S.F. Mertens, M. Ghorbani, M.R. Arshadi, Asymmetrical Schiff bases as inhibitors of mild steel corrosion in sulphuric acid media, Mater. Chem. Phys. 78 (2003) 800-808.

[70] M. Behpour, S. Ghoreishi, N. Mohammadi, M. Salavati-Niasari, Investigation of the inhibiting effect of N-[(Z)-1-phenylemethyleidene]-N-{2-[(2-{[(Z)-1phenylmethylidene] amino} phenyl) disulfanyl] phenyl} amine and its derivatives on the corrosion of stainless steel 304 in acid media, Corros. Sci. 53 (2011) 3380-3387.

[71] M. Morad, A.K. El-'HDQ • -Dithiobis (3-cyano-4, 6-dimethylpyridine): A new class of acid corrosion inhibitors for mild steel, Corros. Sci. 48 (2006) 3398-3412.

[72] Y.H. Kim, S.-G. Roh, S.-D. Jung, M.-A. Chung, H.K. Kim, D.W. Cho, Excited-state intramolecular proton transfer on 2-• -hydroxy-• -R-phenyl) benzothiazole nanoparticles and fluorescence wavelength depending on substituent and temperature, Photochem. Photobiol. Sci. 9 (2010) 722-729.

ACCEPTED MANUSCRIPT

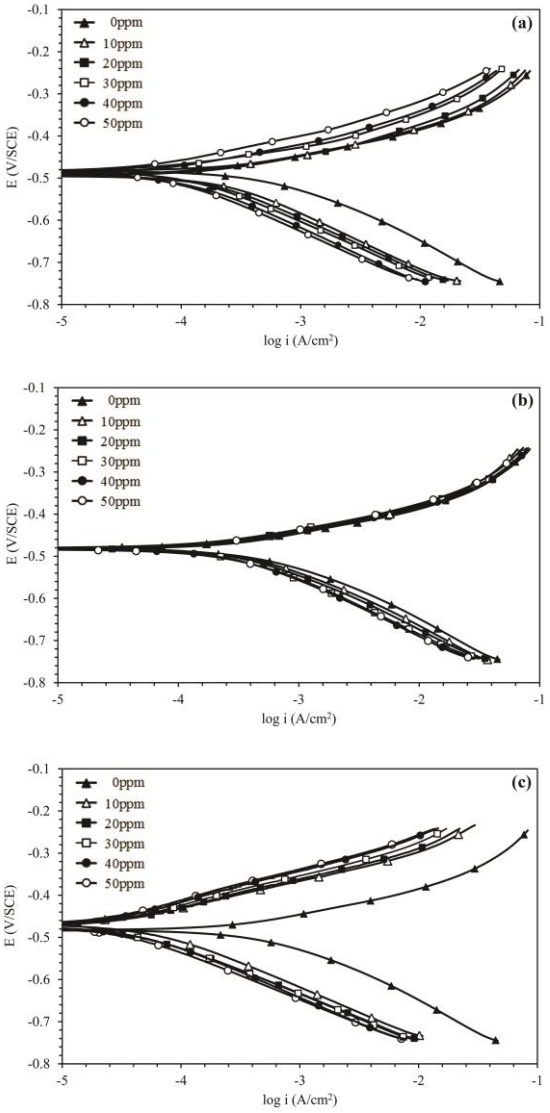

Fig. 1. Potentiodynamic polarization curves of mild steel in 1 M HCl with different concentration of inhibitors at 25 ºC with a scan rate of 1 mV s^{-1}: (a) benzothiazole **1**, (b) benzothiazole **2** and (c) benzothiazole **3**.

ACCEPTED MANUSCRIPT

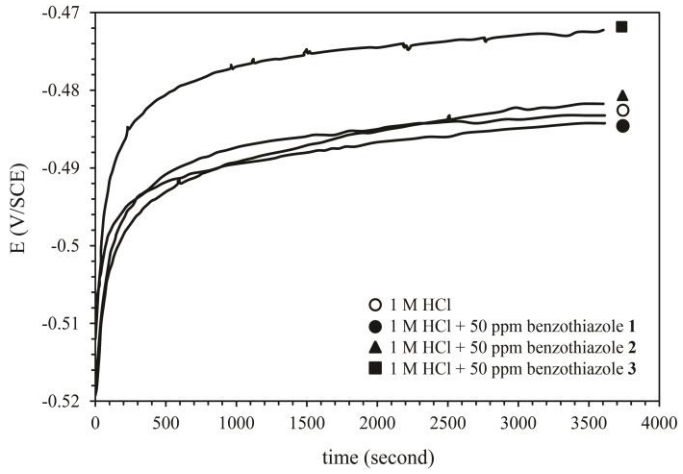

Fig. 2. E_{OCP} versus time curves for mild steel in 1 M HCl at 25 °C solution in absence and presence of 50 ppm (by weight) of inhibitor.

ACCEPTED MANUSCRIPT

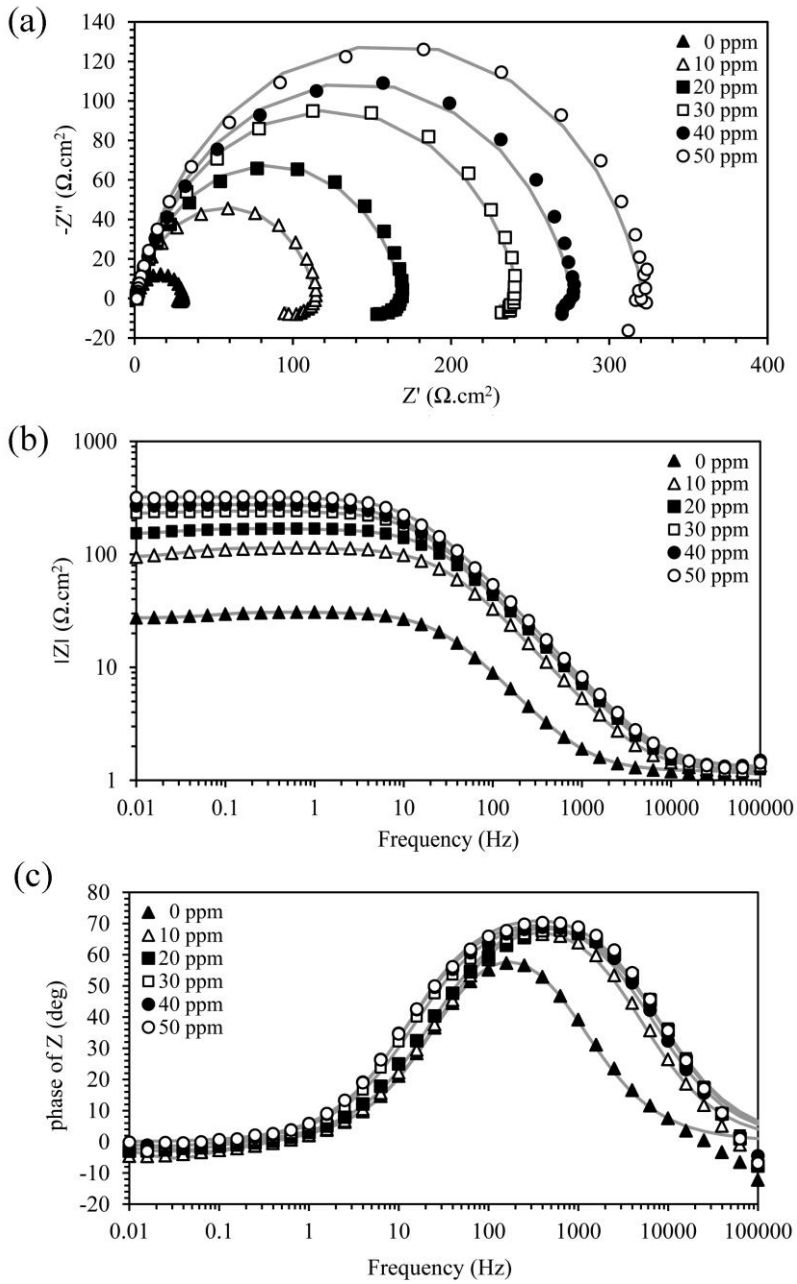

Fig. 3. Electrochemical impedance plots of mild steel in 1 M HCl with 0-50 ppm (by weight) of benzothiazole **1** at OCP and 25 °C: (a) Nyquist, (b) Bode-Z, and (c) Bode-Phase plots (solid lines show fitted results).

ACCEPTED MANUSCRIPT

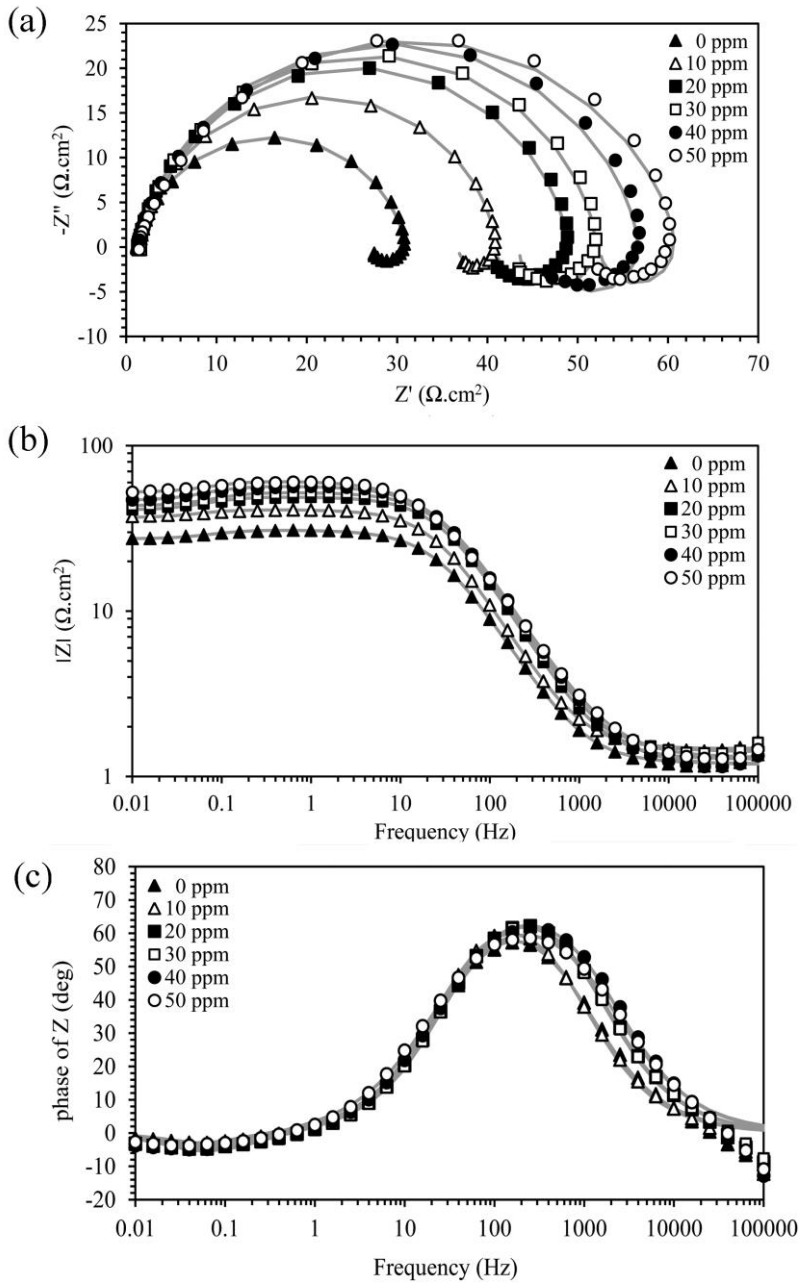

Fig. 4. Electrochemical impedance plots of mild steel in 1 M HCl with 0-50 ppm (by weight) of benzothiazole **2** at OCP and 25 °C: (a) Nyquist, (b) Bode-Z, and (c) Bode-Phase plots (solid lines show fitted results).

ACCEPTED MANUSCRIPT

Fig. 5. Electrochemical impedance plots of mild steel in 1 M HCl with 0-50 ppm (by weight) of benzothiazole **3** at OCP and 25 °C: (a) Nyquist, (b) Bode-Z, and (c) Bode-Phase plots (solid lines show fitted results).

ACCEPTED MANUSCRIPT

Fig. 6. Equivalent circuit used to model metal/solution interface of mild steel in 1 M HCl in the absence and presence of inhibitors (for equivalent circuit diagram, R_s: uncompensated solution resistance, R_{ct}: charge-transfer resistance, Q: constant phase element (CPE), L: inductance, and R_L: inductance resistor).

ACCEPTED MANUSCRIPT

Fig. 7. Variation of the corrosion rate with concentration of the three benzothiazole inhibitors (**1**, **2**, and **3**) for mild steel in 1 M HCl after 16 h immersion at 25 °C.

ACCEPTED MANUSCRIPT

Fig. 8. [illegible] °C at the presence of: (a) benzothiazole **1**, (b) benzothiazole **2** and (c) benzothiazole **3** (is mean values of surface coverage from potentiodynamic polarization measurements).

ACCEPTED MANUSCRIPT

Fig. 9. Optimized structures and the frontier molecular orbital density distributions (HOMO and LUMO) obtained by the B3LYP/6-311G** method of 2-phenyl benzothiazole derivatives **1**, **2** and **3**.

ACCEPTED MANUSCRIPT

Fig. 10. Equilibrium adsorption configurations of 2-phenyl benzothiazole derivatives on the Fe (1 1 0) surface at 298 K obtained by MD simulations: (a and b) **1**, (c and d) **2**, (e and f) **3**.

ACCEPTED MANUSCRIPT

Fig. 11. SEM micrographs of the mild steel surface after 16 h immersion at 25 °C in 1 M HCl: (a) without inhibitor; (b) containing 50 ppm (by weight) benzothiazole **1**; (c) containing 50 ppm (by weight) benzothiazole **2**; (d) containing 50 ppm (by weight) benzothiazole **3**.

ACCEPTED MANUSCRIPT

Table 1. Chemical names, structures, and molecular weight of the three benzothiazole derivatives **1**, **2**, and **3**

Benzothiazole derivative	Structure	Notation	Molecular weight (g mol^{-1})
2-(2-hydroxylphenyl)benzothiazole		**1**	227.28
2-(2,5-dihydroxyphenyl)benzothiazole		**2**	243.28
(4-benzothiazole-2-yl-phenyl)-dimethyl-amine		**3**	254.37

ACCEPTED MANUSCRIPT

Table 2. Electrochemical kinetic parameters extracted from the polarization curves and corresponding inhibition efficiency for mild steel in the absence and presence of 10, 20, 30, 40 and 50 ppm (by weight) of benzothiazole derivatives (**1**, **2**, and **3**) in 1 M HCl at 25 ºC

Inhibitor	C_{inh} (ppm)	E_{corr} vs. SCE (mV)	i_{corr} (µA cm^{-2})	$_a$ (mV dec^{í})	$_c$ (mV dec^{í})	$_p$%	$_p$
-	0	í 482±0.6	435±1.5	122±2.3	í 74±5.6	----	----
1	10	í 494±1.5	217±2.6	133±3.4	í 68±4.6	50	0.50
	20	í 493±0.8	176±3.2	132±6.2	í 66±3.9	59	0.59
	30	í 482±2.3	101±4.6	122±5.4	í 60±3.2	77	0.77
	40	í 490±1.8	88±1.2	123±2.5	í 67±2.6	80	0.8**0**
	50	í 483±0.3	64±2.3	120±4.4	í 71±4.1	85	0.85
2	10	í 480±5.2	350±4.1	127±2.5	í 71±5.2	19	0.19
	20	í 479±3.1	295±3.8	117±4.8	í 59±6.3	32	0.32
	30	í 482±5.2	270±7.1	116±3.3	í 61±3.7	38	0.38
	40	í 482±6.3	250±6.8	126±6.0	í 63±4.9	42	0.42
	50	í 481±7.0	240±8.1	124±5.6	í 66±5.8	45	0.45
3	10	í 491±2.7	49±5.5	110±5.1	í 94±3.7	89	0.89
	20	í 477±1.4	34±2.2	105±5.4	í 77±3.3	92	0.92
	30	í 474±0.9	31±4.7	107±2.7	í 83±5.6	93	0.93
	40	í 470±1.3	27±1.9	111±3.9	í 84±4.7	94	0.94
	50	í 468±0.7	21±5.3	107±4.2	í 80±2.8	95	0.95

ACCEPTED MANUSCRIPT

Table 3. Electrochemical impedance parameters for the corrosion of mild steel in 1 M HCl at open circuit potential with and without different concentrations of benzothiazole derivatives (**1**, **2**, and **3**) at 25 °C

Inhibitor	C_{inh} (ppm)	R_s FP ^{2})	Q		R_{ct} FP ^{2})	R_L FP ^{2})	L (H cm^{-2})	$_{Imp}$%	$_{Imp}$
			Y_0— $^{-1}s^ncm^{-2}$)	n					
-	0	1.19±0.02	381.80±2.3	0.87±0.004	26.20±1.6	3.63±0.3	7.28±0.02	----	----
1	10	1.20±0.02	101.10±3.4	0.87±0.006	93.23±1.4	19.95±0.9	84.92±1.89	72	0.71
	20	1.11±0.04	81.81±2.7	0.86±0.003	150.20±2.5	18.24±0.7	96.71±2.12	83	0.82
	30	1.15±0.01	86.75±5.2	0.85±0.005	239.00±1.7	13.55±0.5	69.25±1.98	89	0.89
	40	1.29±0.02	83.38±1.9	0.85±0.002	275.20±1.9	13.01±0.8	2.73×10^{-13}	90	0.90
	50	1.26±0.03	67.84±6.3	0.86±0.001	320.00±2.3	28.25±1.3	1.60×10^{-12}	92	0.91
2	10	1.47±0.04	282.20±4.3	0.89±0.006	35.29±0.2	12.62±0.7	4.41±0.04	26	0.25
	20	1.27±0.05	212.00±1.2	0.88±0.001	39.71±1.3	18.40±0.9	8.21±0.05	34	0.34
	30	1.41±0.03	195.50±7.9	0.89±0.005	42.03±0.7	16.19±2.3	8.97±0.04	38	0.37
	40	1.18±0.06	215.40±5.6	0.86±0.005	45.61±0.9	23.75±2.9	10.38±0.07	43	0.42
	50	1.30±0.03	277.90±8.1	0.83±0.006	51.18±1.2	18.14±1.5	9.00±0.09	49	0.48
3	10	1.32±0.03	38.89±1.5	0.89±0.002	376.80±2.1	1.08±0.4	41.42×10^{-18}	93	0.93
	20	1.35±0.04	44.44±2.1	0.91±0.003	426.20±2.5	4.83×10^{-3}	2.43×10^{-22}	94	0.93
	30	1.34±0.05	40.79±3.6	0.91±0.003	456.70±3.1	0.35±0.6	1.00×10^{-10}	94	0.94
	40	1.43±0.04	53.87±3.9	0.87±0.001	560.60±3.6	2.84×10^{-5}	1.33×10^{-18}	95	0.95
	50	1.33±0.02	38.86±4.3	0.90±0.004	624.20±2.9	1.39×10^{-15}	2.58×10^{-18}	96	0.95

ACCEPTED MANUSCRIPT

Table 4. Weight loss results of mild steel in 1 M HCl solution after 16 h immersion in the absence and presence of different concentration of the benzothiazole inhibitors (**1**, **2**, and **3**) at 25 °C

Inhibitor	**C_{inh} (ppm)**	**C_{RW} (mm y^{-1})**	**$_{w}$%**
-	0	127.9±0.3	-
1	10	63.1±0.4	50.3
	20	51.7±0.3	59.4
	30	21.0±0.2	83.5
	40	13.1±0.6	89.4
	50	10.5±0.2	92.1
2	10	104.2±0.8	18.7
	20	81.5±0.5	36.1
	30	78.0±0.7	39.0
	40	69.2±0.3	45.7
	50	62.2±0.4	51.6
3	10	23.7±0.4	81.5
	20	18.4±0.6	85.6
	30	10.5±0.3	92.0
	40	6.1±0.3	94.8
	50	4.4±0.2	96.8

ACCEPTED MANUSCRIPT

Table 5. Standard thermodynamic and equilibrium adsorption parameters for adsorption of benzothiazole derivatives (**1**, **2**, and **3**) on mild steel surface in 1 M HCl solutions at 25 °C

Inhibitor	K_{ads} (L mol^{-1})	ΔG°_{ads} (kJ mol^{-1})
1	18.62×10^{3}	±34.31
2	6.95×10^{3}	±31.87
3	256.41×10^{3}	±40.80

ACCEPTED MANUSCRIPT

Table 6. Calculated quantum chemical parameters of benzothiazole derivatives (**1**, **2**, and **3**) obtained from the B3LYP/6-311G** method

Parameters	Inhibitors		
	1	**2**	**3**
E_{HOMO} (eV)	-6.2719	-6.0017	-5.4200
E_{LUMO} (eV)	-1.6541	-1.6897	-1.5112
' E(eV)	4.6178	4.3120	3.9088
P (D)	1.7845	2.3424	4.1134
û	0.6576	0.7017	0.9042

ACCEPTED MANUSCRIPT

Table 7. The output obtained from MD simulations for the adsorption of benzothiazole derivatives (**1**, **2**, and **3**) on the Fe (1 1 0) surface at 298k

Systems	$E_{intraction}$ (kJ mol^{-1})	$E_{binding}$ (kJ mol^{-1})
Fe (1 1 0) + **1**	í 550.36	550.36
Fe (1 1 0) + **2**	í 528.13	528.13
Fe (1 1 0) + **3**	í 622.98	622.98